Joint time-frequency and finite-difference time-domain analysis of precursor fields in dispersive media

Reza Safian, Costas D. Sarris, and Mohammad Mojahedi
The Edward S. Rogers, Sr. Department of Electrical and Computer Engineering, University of Toronto, Toronto, Ontario, M5S 3G4, Canada

(Received 6 June 2005; revised manuscript received 2 February 2006; published 2 June 2006)

Superluminal group velocities, defined as group velocities exceeding the speed of light in vacuum, c, have been theoretically predicted and experimentally observed in various types of dispersive media, such as passive and active Lorentzian media, one-dimensional photonic crystals, and undersized waveguides. Though superluminal group velocities have been found in these media, it has been suggested that the pulse "front" and associated transient field oscillations, known as the precursors or forerunners, will never travel faster than c, and hence relativistic causality is always preserved. Until now, few rigorous studies of these transient fields in structures exhibiting superluminal group velocities have been performed. In this paper, we present the dynamic evolution of these earliest field oscillations in one-dimensional photonic crystals (1DPC), using finite-difference time-domain (FDTD) techniques in conjunction with joint time-frequency analysis (JTFA). Our study clearly shows that the precursor fields associated with superluminal pulse propagation travel at subluminal speeds, and thus, the arrival of these precursor fields must be associated with the arrival of "genuine information." Our study demonstrates the expected result that abnormal group velocities do not contradict Einstein causality. This work also shows that FDTD analysis and JTFA can be combined to study the dynamic evolution of the transient and steady state pulse propagation in dispersive media.

DOI: 10.1103/PhysRevE.73.066602 PACS number(s): 42.25.Fx, 02.70.Bf, 73.40.Gk

I. INTRODUCTION

Wave propagation in dispersive media has been a complex and sometimes controversial research topic since the late 19th century. Sommerfeld and Brillouin were among the early researchers studying wave propagation in linear, homogeneous, isotropic, causally dispersive media [1]. They used the asymptotic method of steepest descent to describe the propagation of a unit step-modulated signal with a constant carrier frequency in a semi-infinite, single resonance, passive Lorentz medium. The purpose of their analysis was to find the velocity at which the "signal" propagated. Their analysis led to the discovery of two wave phenomena that precede the main signal in a dispersive medium, which they named "forerunners" or "precursors." The first precursor (Sommerfeld's precursor) determines the earliest-time behavior of the signal, and contains its highest frequency components. The second precursor (Brillouin's precursor) contains the lowest frequency components of the signal. Sommerfeld also found that the front of the pulse—that is, the moment when the field first becomes nonzero—propagates precisely at c. He stressed that a very sensitive detector should be able to register the front of the pulse and hence measure a propagation speed of c for the signal, independent of the medium in which the signal is propagating.

Sommerfeld and Brillouin's classification of different wave velocities—into phase, group, energy, and precursor velocities—continues to be the standard. It has been argued that all these velocities, except the precursor's, can exceed c or become negative in special circumstances [2]. Superluminal or negative group velocities have been demonstrated in experiments at microwave frequencies [3–8], at optical frequencies [9,10], in the single-photon limit [11,12], and even in media with a negative index of refraction [13,14]. Since these abnormal group velocities can be measured, we must question the traditional notion that, in regions near resonances, group velocity "no longer [has] any appreciable physical significance" [15] or "ceases to have a clear physical meaning" [16]. Despite one's initial impression, superluminal, or negative group velocities are not at odds with the requirements of relativistic causality, and indeed, it can be shown that they must exist as a consequence of the Kramers-Kronig relations, which themselves are a statement of the system linearity and causality [17–20].

In a causal, dispersive medium, the signal arrival is indicated by the field amplitude increasing from the precursor field level to the level of the steady-state signal. As mentioned before, among all the aforementioned velocities, it is only the "front" velocity alone that must satisfy the requirements of Einstein causality. In other words, Einstein causality does not always equate the group velocity with the velocity of information transfer, particularly when propagation of attenuated traveling waves is involved. Therefore, a correct description of the signal arrival requires a correct analysis of the precursor fields and their role in the dynamic evolution of the field. Oughstun and co-workers have done extensive work on precursors in Lorentzian media by refining and generalizing Sommerfeld and Brillouin's results [21]. Surprisingly, there has been little work on the precursors in dispersive, non-Lorentzian media; particularly, no research has addressed precursor velocities in media that exhibit abnormal group velocities due to structural dispersion—that is, dispersion due to geometrical features—such as Bragg reflectors and photonic crystals.

This paper is organized as follows. In Sec. II a brief description of the finite-difference time-domain (FDTD) algorithm and joint time-frequency analysis (JTFA) is provided. In Sec. III, we use the combined FDTD and JTFA to study

the evolution of the precursors in a single resonance Lorentzian medium subject to a modulated Gaussian excitation. Our results agree very well with the results obtained from the asymptotic analysis of [22]; this agreement reinforces the conclusion that combining FDTD and JTFA provides a robust and versatile method for studying the precursor fields in complex structures such as 1DPC. In Sec. IV, we present the superluminal propagation of a modulated Gaussian pulse inside a 1DPC with various conditions on the front. These simulations confirm that the front travels with a speed very close to the speed of light. It is also shown that the attenuation rate for the precursors is lower than the attenuation of the rest of the pulse, hence providing the possibility of further penetration into the dispersive medium. Section V summarizes our final thoughts.

II. FDTD AND JOINT TIME-FREQUENCY ANALYSIS (JTFA)

The dynamical structure of the propagated field in a simple dispersive medium such as single resonance Lorentzian may be obtained through the evolution of the saddle points associated with the complex phase function. This asymptotic theory provides a relatively good approximation of the pulse propagation in dispersive media with good physical insights of the time and frequency evolution of the signal. On the other hand, numerical techniques such as FDTD offer an accurate description of pulse propagation in time domain in both simple and complex dispersive media [23]. The drawback to FDTD as a time-domain technique is that it provides little physical insight into the frequency evolution of the signal that is important in studying a dispersive medium. However, the signal processing technique of JTFA can be used as a post-processing tool to restore the loss of this insight by retrieving the frequency evolution of the signal from the time-domain data. Therefore, the combination of FDTD and JTFA is a viable tool for studying the time and frequency evolution of the signal inside a complex dispersive medium.

The FDTD method solves Maxwell's equations by approximating the curl equations using centered finite differences for both the temporal and spatial derivatives, and then marches the fields through time to obtain transient results directly. The FDTD results are full-wave solutions of the wave equation, using a fine discretization in time and space guarantees the accuracy of the results [23]. Lorentzian dielectric media are modeled via the so-called auxiliary differential equation (ADE) technique [23]. Throughout the paper, one-dimensional wave propagation along the x-axis is assumed and numerical calculations are aimed at the iterative determination of the E_z and H_y field components, while the use of the constitutive relation between D_z and E_z accounts for dispersive effects. Space and time are discretized in steps Δx and Δt, respectively, related with each other through the Courant stability criterion $c\Delta t/\Delta x \leqslant 1$. In the following calculations, this ratio (also referred to as the Courant stability number) has been chosen to be 0.9. Typically, the choice of the space step Δx is dictated by the need to guard against the pronounced numerical dispersion-induced errors that FDTD suffers from. To that end, the choice of a space step that would be a tenth of a wavelength or less is necessary. This condition has been fulfilled at all stages of this work, since our interest in determining the impact of the spectral tail of a pulse excitation on the transient response of Lorentzian and composite dielectric media has forced us to choose much denser spatial discretization rates than the ones normally employed. Therefore, numerical dispersion effects, arising in the FDTD modeling of dielectric media [24], are kept to negligibly small levels.

An interesting question, that FDTD by itself cannot address, is what frequency components of the signal give rise to the fields at each point in time. A natural way to address this question is to use the signal-processing technique of JTFA [25]. Joint time-frequency distributions of signals provide the temporal localization of the frequency components of a signal. Considered as such, JTFA has the ability to relate the frequency content of a pulse propagating in a dispersive medium to its temporal evolution and it can be used as a systematic numerical method to identify the Sommerfeld and Brillouin precursors as the products of the high and low frequency components of the signal. In the field of computational electromagnetics, JTFA has been mainly employed for remote sensing and scattering problems [26,27].

Linear time-frequency distributions such as the short time Fourier transform (STFT) and the wavelet transform, and quadratic time-frequency distributions such as the spectrogram, the Page distribution, and the Wigner-Ville distribution (WVD) are the two main categories of joint time-frequency distributions available. In linear distributions, signal is distributed linearly along the two variables of time and frequency. Therefore, as a consequence of the Heisenberg inequality, there is a tradeoff between the time and frequency resolutions. On the other hand, in quadratic distributions, energy of the signal is distributed between the two variables of time and frequency. Thus both time and frequency resolutions can be granted at the same time. The drawback is the presence of the cross terms that are inherent to the quadratic distributions. Due to the fast-varying nature of the precursors in time and frequency, a joint time–frequency distribution with high resolution in both time and frequency is needed to correctly characterize the evolution of the precursors. Therefore, to study the precursors, quadratic distributions are definitely a better choice than the linear distributions. Among all possible quadratic distributions, WVD is chosen because it provides relatively high resolution in the time-frequency plane, a consequence of the fact that it has the highest signal concentration on that plane [25]. The WVD of a signal $x(t)$, with a Fourier transform $X(f)$ can be defined either as:

$$W_x(t,f) = \int_{-\infty}^{+\infty} x(t+\tau/2)x^*(t-\tau/2)\exp(-i2\pi f\tau)d\tau, \quad (1)$$

or as:

$$W_x(t,f) = \int_{-\infty}^{+\infty} X(f+\xi/2)X^*(f-\xi/2)\exp(-i2\pi\xi t)d\xi, \quad (2)$$

where * denotes complex conjugate. While WVD gives the best resolutions in time and frequency, as stated previously,

the drawback is the relatively large interference terms present in the distribution. These can be troublesome, since they may overlap with the signal and thus make it difficult to visually interpret the WVD image. However, it appears that these terms must be present for the good properties of the WVD (marginal properties, instantaneous frequency, group delay, and so on) to be present. The interference terms are rather easily (visually) recognizable due to their discontinuous structure. Moreover, these interference terms do not appear in the steady-state representations of the signal; therefore, Fourier transform of the signal can also be used to identify the cross terms.

III. ULTRA SHORT MODULATED GAUSSIAN PULSE PROPAGATING IN A SINGLE RESONANCE LORENTZIAN MEDIUM

As mentioned previously, most of the studies of the precursor fields have been concerned with the pulse propagation in a Lorentzian medium. In these situations, the application of the asymptotic analysis to the integral representation of the wave propagation, results in a dynamic description of the propagating pulse. The integral representation of the propagated plane wave in the half space $z \geqslant 0$ is given by

$$A(z,t) = \frac{1}{2\pi}\int_C \tilde{f}(\omega)\exp\left[\frac{z}{c}\phi(\omega,\theta)\right]d\omega, \tag{3}$$

where $\theta = ct/z$ is a dimensionless space-time parameter and

$$\phi(\omega,\theta) = i\omega[n(\omega) - \theta], \tag{4}$$

is the complex phase function. The function $A(z,t)$ represents any scalar component of the electric field $[E(z,t)]$ or magnetic field $[H(z,t)]$. Here, $\tilde{f}(\omega)$ is the Laplace transform of the initial pulse $f(t)=A(0,t)$ at the input plane. The spectral amplitude of $A(z,t)$ [i.e., $\tilde{A}(z,\omega)$] satisfies the scalar Helmholtz equation

$$[\nabla^2 + \tilde{k}^2(\omega)]\tilde{A}(z,\omega) = 0, \tag{5}$$

with complex wave number $\tilde{k}(\omega) = \omega n(\omega)/c$. In order for the integral in (3) to be convergent, contour of integration C is taken to be a straight line $\omega = \omega' + ia$ on the complex ω-plane, with a being a fixed positive constant that is greater than the abscissa of convergence of the function $\tilde{f}(\omega)$ [28,29].

In the following, we have used the FDTD method in conjunction with Wigner-Ville JTFA to study the precursor fields in a Lorentzian medium. These results—which are in excellent agreement with the Oughstun *et al.* asymptotic analysis [21,22]—further underline the correctness and the versatility of the combined FDTD and JFTA, as a tool in studying the dynamic evolution of the precursor fields, particularly when it is applied to a more complicated structure such as the 1DPC of the next section. We consider the propagation of a modulated Gaussian pulse inside a passive Lorentzian medium that occupies the half-space $z \geqslant 0$. The input modulated Gaussian pulse propagating in the positive z direction is given by

$$S(t) = \exp\left[-\left(\frac{t-t_0}{T_s}\right)^2\right]\sin(\omega_c t), \tag{6}$$

where ω_c is the carrier frequency and the pulse is centered around the time $t_0 > 0$ at the $z=0$ plane with a full width at $1/e$ point given by $2T_s$. The medium is characterized by a single Lorentzian resonance with complex index of refraction

$$n(\omega) = \left(1 - \frac{\omega_p^2}{\omega^2 - \omega_0^2 + 2i\delta\omega}\right)^{1/2}, \tag{7}$$

Here, ω_0 is the resonance frequency, ω_p is the plasma frequency, and δ is the damping constant of the dispersive, lossy dielectric. The material absorption band is defined over the approximate angular frequency domain $(\sqrt{\omega_0^2 - \delta^2}, \sqrt{\omega_1^2 - \delta^2})$, where $\omega_1 = \sqrt{\omega_0^2 + \omega_p^2}$. The material dispersion is normal ($n_r(\omega)$ increases with increasing frequency) over the approximate angular frequency domains $[0, \sqrt{\omega_0^2 - \delta^2}]$ and $[\sqrt{\omega_1^2 - \delta^2}, \infty]$, below and above the absorption band, respectively, while it is anomalous ($n_r(\omega)$ decreases with increasing frequency) over the approximate angular frequency domain $[\sqrt{\omega_0^2 - \delta^2}, \sqrt{\omega_1^2 - \delta^2}]$ containing the absorption band.

The Brillouin choice of medium parameters which describes a highly absorptive material is used in the numerical calculations ($\omega_0 = 4\times10^{16}$ Hz, $\delta = 0.28\times10^{16}$ Hz, and $\omega_p = 4.47\times10^{16}$ Hz). The modulated Gaussian pulse with parameters $\omega_c = 5.75\times10^{16}$ Hz, $T_s = 1$ fs, and $t_0 = 3\times T_s$ is a wideband pulse that its frequency distribution covers the anomalous dispersion region of the medium. We have used the space and time discretization parameters, $\Delta x = \lambda/400$ and $\Delta t = s\Delta x/c$, where λ is the wavelength at the carrier frequency of the modulated pulse and $s = 0.9$ is the Courant stability number.

Since the input carrier frequency ω_c lies within the medium absorption band, the frequency components of the propagating field that are within this band will be significantly attenuated. As the consequence of propagation, the input Gaussian evolves into two Gaussian-shaped pulses, the first containing the high-frequency oscillations, while the second pulse contains the low-frequency oscillations. These first and second pulses are recognized as the Sommerfeld and Brillouin precursors, respectively.

Figures 1 and 2 show the time and frequency evolution due to the input Gaussian pulse at propagation distances $z = 0.5$ μm and $z = 1$ μm, respectively. The high frequency oscillations in the beginning of the time distribution of the signal in Fig. 1(a) is the Sommerfeld precursor that has completely evolved. The oscillations following the Sommerfeld precursor are part of the Brillouin precursor that has not completely evolved at this observation point. The JTFA in Fig. 1(b) shows that the frequency evolution of the Sommerfeld precursor begins with high frequencies that are above the absorption band and decreases as θ' ($\theta' = \theta - ct_0/z$) increases. At one point around $\theta' = 1.5$ the frequency begins increasing towards the carrier frequency from below the ab-

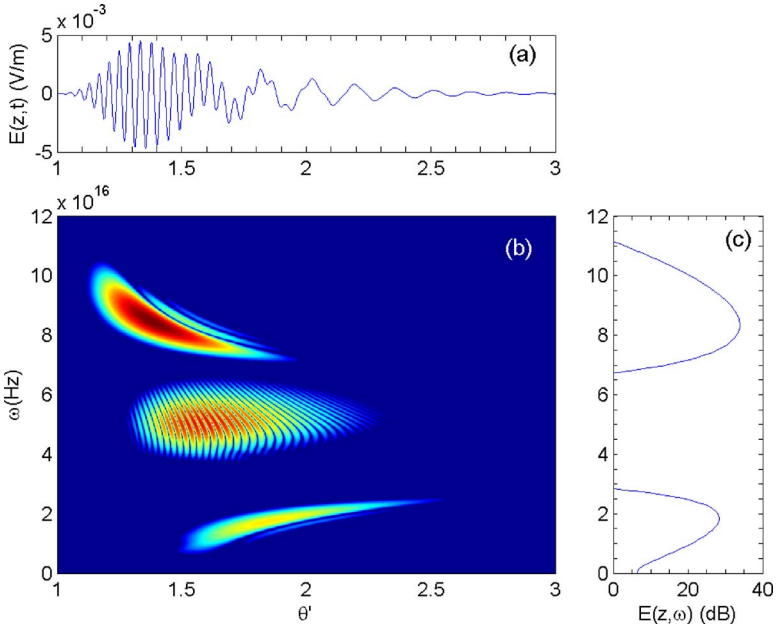

FIG. 1. (Color online) (a) Time distribution, (b) joint time-frequency distribution, (c) frequency distribution of the modulated Gaussian pulse after propagating 0.5 μm through the dispersive Lorentzian medium. ($\theta' = \theta - ct_0/z$).

sorption band due to the Brillouin precursor. In Fig. 2 the pulse has traveled deeper inside the medium and both Sommerfeld and Brillouin precursors are fully present. The Sommerfeld precursor has similar frequency evolution as in Fig. 1, and around $\theta' = 1.5$ the Brillouin precursor appears, where its frequency evolution starts from low frequencies and increases towards the carrier frequency. In both JTFA plots, there are high intensity components in the absorption band. These components are the superfluous cross terms in the WVD. As stated earlier, to have a good frequency resolution these cross terms are unavoidable. However, these cross terms in the absorption band can be simply identified from their oscillatory appearance. Integrating these cross-terms over frequency results to zero, as shown from the absence of frequency components of the signal in the band. The bandwidth and resolution of the JTFA is necessarily limited by those of the FDTD technique. However, the FDTD bandwidth is chosen to be wide enough to include the spectral content of the excitation pulse up to frequencies with a power spectral density that is 30 dB lower than its maximum.

The results presented here are in good agreement with those calculated using asymptotic techniques in [22]. Our results show that a combination of FDTD as a time domain technique, and JTFA as a post processing technique can be used to provide a comprehensive view of the pulse evolution in both time and frequency domains.

IV. PRECURSORS IN A ONE-DIMENSIONAL PHOTONIC CRYSTAL (1DPC)

So far, most studies of the precursor fields have been concerned with Lorentzian media with little or no attention be-

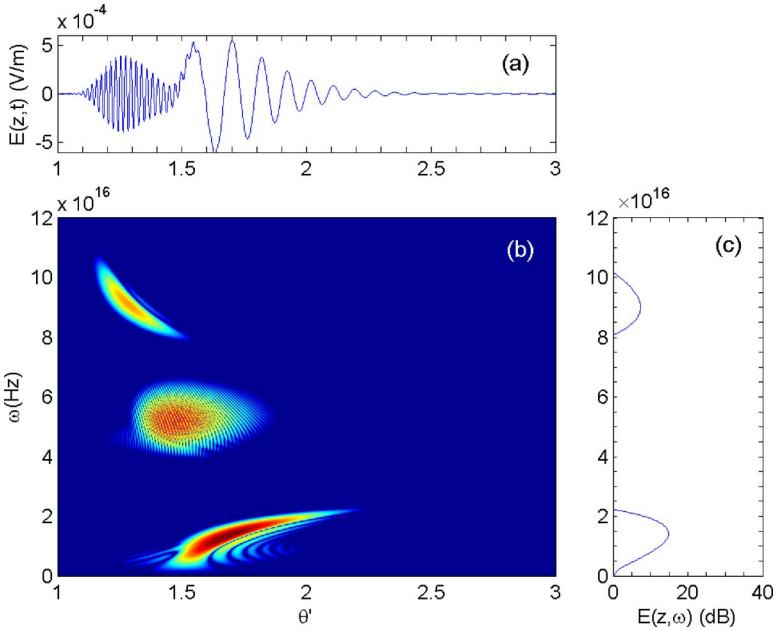

FIG. 2. (Color online) (a) Time distribution, (b) joint time-frequency distribution, (c) frequency distribution of the modulated Gaussian pulse after propagating 1 μm through the dispersive Lorentzian medium. ($\theta' = \theta - ct_0/z$).

ing paid to a more complex structure such as 1DPC. This is partially due to difficulties in applying the asymptotic analysis to these structures. The results from the previous section show that a combination of FDTD and JTFA can be used as a robust and accurate tool to study the precursors (or in general the transient response) in any dispersive media including 1DPC. In this section, this combination has been used to study the wave propagation in a 1DPC exhibiting superluminal group velocities. In an inhomogeneous structure such as 1DPC it is the multiple reflections that make up the medium response. Superluminal group velocity in 1DPC has been experimentally verified in several experiments. For example, in a series of experiments Chiao *et al.* have measured the group velocity of a single-photon wave packet traversing a 1DPC. The photon frequency was chosen to correspond to the frequency at the center gap, and although the tunneling appeared to be superluminal, they argued that it was a causal effect resulting from the pulse reshaping processes [17]. In the microwave domain, Mojahedi *et al.* have measured superluminal group velocity for the wave propagation through the bandgap of a 1DPC [30].

In the following, we have analyzed the superluminal propagation of a modulated Gaussian pulse through a 1DPC. The geometry of the 1DPC is based on the physical experiment by Mojahedi *et al.* [30]. It consists of five dielectric slabs with the width of 1.27 cm. The slabs are separated by 4.1 cm air-gaps. The dielectric model in the 1DPC is a single Lorentzian with parameters $\omega_0=4\times10^{11}$ Hz, $\delta=0.28\times10^{11}$ Hz, and $\omega_p=4.47\times10^{11}$ Hz. We have used the space and time discretization parameters, $\Delta x=\lambda/50$, $\Delta t=s\Delta x/c$ where λ is the wavelength at the resonance frequency of the medium and $s=0.9$ is the Courant stability number. Due to the fine discretization of the medium in 1DPC the abrupt change of the dielectric constant at the air-dielectric slab interfaces does not contribute significant numerical errors. The structure is excited with a modulated Gaussian pulse with parameters $f_c=9.6$ GHz, $T_s=3.11$ ns, and $t_0=3\times T_s$. The center frequency of the modulated Gaussian is inside the bandgap of the 1DPC. Since the important frequency components of the pulse are inside the bandgap, the contributions of the frequency components outside the bandgap are negligible. Figure 3 shows the pulse that has traveled the same distance through the 1DPC and free space. The peak of the pulse that has traveled through the 1DPC appears in the output 479 ps sooner than the companion pulse traveling through free space, attenuated by about 14 dBs.

The group velocity of the pulse propagating through the 1DPC of length L_{pc} is given by

$$v_g = L_{pc}/\tau_g, \tag{8}$$

where τ_g is the time associated with traversing the 1DPC, also known as group delay. Fundamentally, it is the transmission function of the structure that defines the group delay and it is related to the frequency derivative of the transmission phase, $\mathrm{Arg}[T(\omega)]$ as:

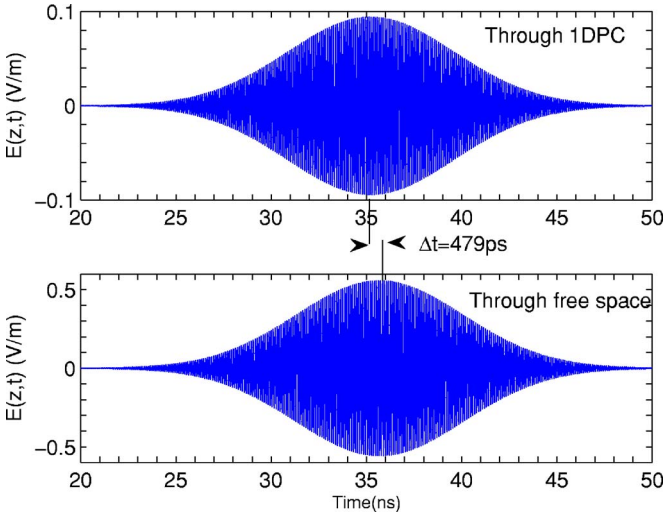

FIG. 3. (Color online) Pulse advancement in the 5-slab 1DPC.

$$\tau_g = \frac{\partial\,\mathrm{Arg}(T(\omega))}{\partial\omega}. \tag{9}$$

The time difference between the peaks of the pulses that have traveled through 1DPC and free space (Δt) can be used to calculate the group delay according to

$$\tau_g = \frac{L_{pc}}{c} - \Delta t. \tag{10}$$

The length of the 1DPC is $L_{pc}=22.75$ cm and based on the simulation results $\Delta t\simeq479$ ps; therefore, group velocity in the 1DPC is $v_{pc}=2.7c$.

The excitation in Fig. 3 has a very smooth turn-on (the amplitude of the pulse at the turn-on point is e^{-9}, whereas the peak amplitude is unity). Figure 4 shows the Wigner-Ville distribution of the aforementioned smooth

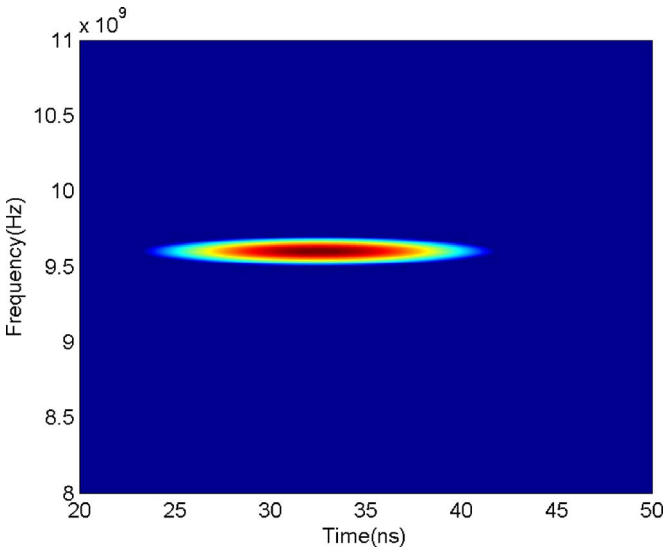

FIG. 4. (Color online) Wigner-Ville distribution of the output pulse with the smooth front excitation in the 5-slab 1DPC.

pulse propagated through the 1DPC. It is similar to the time-frequency distribution of the pulse that has propagated in free space with Gaussian distribution both in time and frequency.

The interesting question is whether or not the abnormal behavior observed in Fig. 3 is consistent with the requirements of special relativity, which demands no information to be transmitted faster than the speed of light in vacuum. It has been argued that if an information-carrying signal is to be presented as an entire function (function that is analytic on the whole complex plane) extending in time from $-\infty$ to $+\infty$, then by definition the signal possesses an infinite number of derivatives and the future and early behavior of the pulse can be predicted by using Taylor expansion about any point in time ([30] and references therein). Therefore, a signal without any turn-on point does not convey "genuine" information. Furthermore, an information-carrying signal that is physically realizable is a causal signal that has a beginning in time and space ("front"). Consequently, in a noiseless channel (as we have considered in all the simulations), the earliest time that the future value of the information carrying signal can be predicted is $t=0^+$, since $t=0$ by definition is a point of nonanalyticity for which the Taylor expansion does not exist. Therefore, the genuine information regarding the correct value of a causal signal is contained within the time interval beginning with $t=0$ (the "front") and times immediately following it (precursors).

Simulations in Fig. 3 were obtained for a pulse with a very smooth front where the effects of the front are not easily observed at the output. To observe the evolution of the front, we have explicitly introduced an excitation that enforces the front. For this excitation, a second-order nonanalyticity has been introduced in the beginning of the pulse used in the prior simulations. The excitation is zero at $t=0$, and the amplitude of the pulse increases smoothly with time (the envelope is a second order polynomial) and at the point that the amplitude of the pulse reaches $e^{-2.25}$ (where the maximum of the pulse is unity) the second-order nonanalyticity is introduced by matching the second-order polynomial envelope and the Gaussian envelope with parameters; $T_s=3.11$ ns, $t_0=1.5\times T_s$. Figure 5(a) shows the envelope of this excitation and the excitation with a smooth turn-on [$E_2(t)$ and $E_1(t)$, respectively] and Fig. 5(b) shows the frequency distribution of this pulse compared to the frequency distribution of the excitation with the smooth turn-on [$E_2(f)$ and $E_1(f)$, respectively]. Comparing the frequency distributions of the two pulses shows that introducing the strong front adds small amplitude, low and high frequency components (with respect to the center frequency) to the frequency distribution of the pulse with a smooth turn-on. The spectral content of these frequencies can be controlled by the order of nonanalyticity introduced. A higher order nonanalyticity renders the beginning of the signal smoother and reduces the high-frequency content of the associated precursor fields. Input reflection (S_{11}) of the 5-slab 1DPC calculated using FDTD is also shown in Fig. 5(b). Comparing the frequency distribution of the excitation pulses to the S_{11} shows that the frequency distribution of both pulses, with and without enforced front, is still narrower than the stop-band of the 1DPC; hence, the steady-state dispersion mechanism is similar for both excitations.

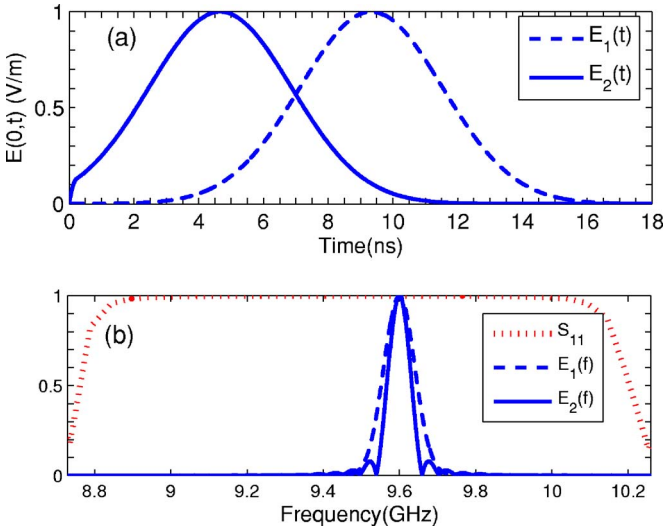

FIG. 5. (Color online) (a) Envelope of the modulated Gaussian excitation with [$E_2(t)$] and without [$E_1(t)$] enforced front. (b) Input reflection coefficient (S_{11}) of the 5-slab 1DPC and frequency distribution of the excitations with [$E_2(f)$] an without [$E_1(f)$] enforced front.

Figure 6 shows the pulse with enforced front that has propagated through a 1DPC with 5 slabs and its Wigner-Ville distribution. There are some cross-terms in Fig. 6 that appear as discontinuous, symmetrical lines around the center frequency. The only difference between the output pulse of the 5-slab 1DPC in this simulation with enforced front and the output pulse in the previous simulation with smooth front is the oscillations ("precursors") in the early part of the pulse. The maximum amplitude of these early oscillations is comparable to the maximum of the main pulse and they have a Gaussian-type envelope. The JTFA shows that these precursors include high and low frequencies that are not present in the remaining part of the pulse and the low and high frequencies appear simultaneously in the beginning. The fact that

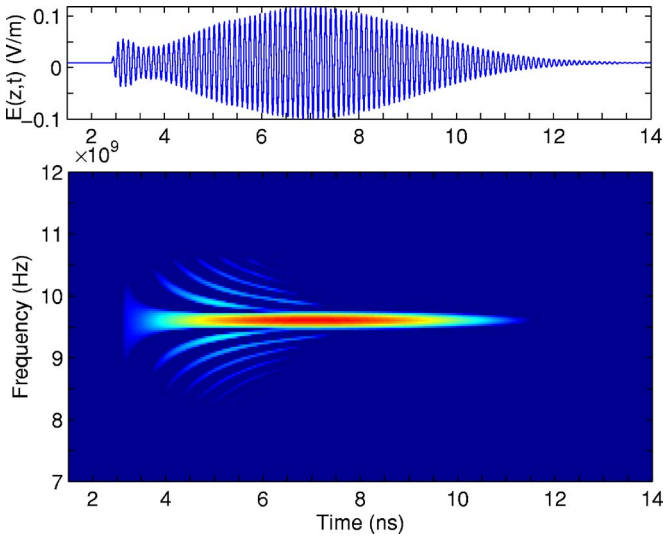

FIG. 6. (Color online) Wigner-Ville distribution of the output pulse with the enforced front excitation in the 5-slab 1DPC.

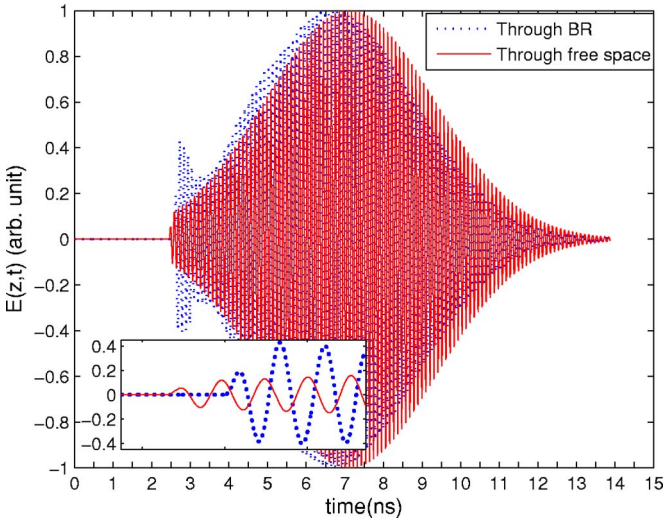

FIG. 7. (Color online) Normalized Gaussian pulse with enforced front at the output of the 1DPC compared to the same pulse that has traveled the same length in free space.

these frequencies have a continuous structure indicates that they do not correspond to cross-terms.

Figure 7 shows that the peak of the pulse that has traveled through the 1DPC appears in the output sooner than the peak of the pulse that has traveled through free space. The advancement is approximately 495 ps, which is close to the advancement of the pulse with a smooth front. As mentioned earlier, group velocity is governed by the transmission function of the 1DPC [Eq. (9)]. It can be seen in Fig. 5(b) that the frequency distribution of both pulses, with and without enforced front, are inside the bandgap of the 1DPC; therefore, the same steady-state mechanism applies to both of them and the advancement in both cases is similar.

An interesting observation is that although the group velocity is superluminal, it can clearly be seen in the Fig. 7 inset that the early oscillations of the pulse that has traveled through the 1DPC appear with a negligibly small delay compared to the early oscillations of the pulse that has traveled through the free-space. This effect can be explained as follows. As a causal signal, the excitation used in our FDTD simulations contains an unbounded spectrum of frequencies. The front of the pulse, which is formed from large frequency signal harmonics, will encounter an index of refraction close to 1, effectively propagating as in a vacuum. This is in agreement with the Sommerfeld and Brillouin results. In this experiment, the time it takes the front to propagate through the 1DPC (L_{pc}=28.77 cm) is 0.964 03 ns and the time it takes the front to travel through the same length in free space is 0.959 70 ns. Based on these calculations we can define an effective 1DPC index for the front (n_{eff}=1.0045), which, as expected, is very close to the index of the free space.

If one would model the dielectric slabs of the 1DPC as possessing a dispersionless refractive index, the front would appear to propagate with a subluminal velocity [31]. However, this would be a side effect of neglecting dispersion and hence enforcing the propagation of the front through an effective medium composed of the combination of the dielectric slabs and free space, with an effective index that can be defined as:

$$n_{ave} = ct_{ave}/L_{pc}, \tag{11}$$

where

$$t_{ave} = l_s/(c/n) + l_a/c. \tag{12}$$

In the latter, l_s and l_a are the total lengths of dielectric and air regions through which the pulse propagates, while n=1.66 is the assumed dielectric slab index. As a result, based on the 1DPC parameters in [31], the average index is n_{ave}=1.0495. We can also calculate n_{ave}, which is defined as

$$n_{ave} = ct_{pc}/L_{pc} \tag{13}$$

from the FDTD results, where t_{pc} is the time it takes the pulse to propagate from the source and the observation point. In the numerical results of [31], t_{pc}=2.9079 ns and L_{pc}=83.05 cm. Therefore, n_{ave}=1.0503, which is very close to the value that was calculated numerically.

To further study the propagation of the front inside the photonic crystal in another series of simulations, a 1DPC with the same parameters as the previous simulations but with different number of slabs has been considered. Increasing the number of slabs slightly changes the dispersion characteristics of the structure and increases the attenuation of the signal. Consequently, by increasing the number of slabs we can study the attenuation rate of different portions of the pulse. Figure 8 shows the output pulses for a 1DPC with different number of slabs. It clearly shows that attenuation is not the same for different parts of the pulse, and as the number of slabs is increased, the precursor begins to separate from the remaining part of the pulse. In the 5-slab 1DPC, the amplitude of the precursor is lower than the main part of the pulse, but as the number of slabs increases to 9, the amplitude of the precursor grows larger than the main pulse. In other words, the decay rate for the precursor is smaller than the decay rate for the main pulse. For a 1DPC with 9-slab, the Gaussian pulse has completely lost its coherence and does not have any distinct maximum, while the precursor still has its initial Gaussian-type shape. Another important observation about the precursors is that in contrast with the main part of the signal that has a constant delay, their delay increases with the number of the slabs. The reason that the delay of the main part of the pulse remains almost constant is that its frequency content is inside the bandgap of the 1DPC, where its phase advancement is close to zero. On the other hand, the evolution of the precursors takes place at a transient stage, where this bandgap is still under formation, therefore allowing for a nonzero delay of the precursors as they travel through the 1DPC.

Using the information in Fig. 8, we can compare the behavior of the precursor and main part of the pulse in terms of energy. To do this, we have used the term U, which is proportional to energy of the signal, and it is defined as

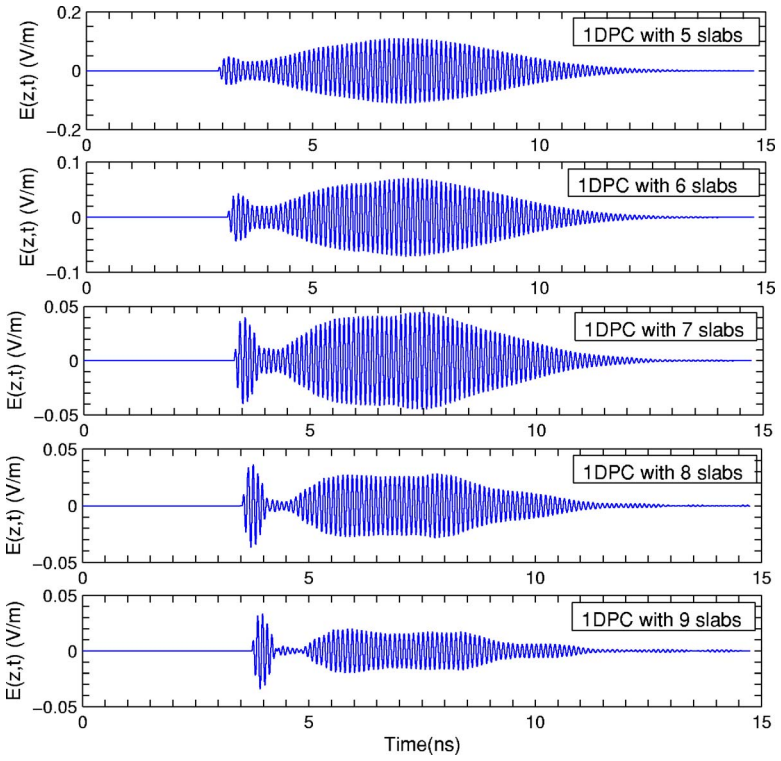

FIG. 8. (Color online) Propagation of the Gaussian pulse inside the 1DPC with different number of slabs.

$$U = \int_{t_1}^{t_2} |E(z = L_{pc}, t)|^2 dt. \tag{14}$$

Figure 9 shows the values of U that havebeen calculated using the output signals in Fig. 8. The time spots t_1 and t_2 in (14) are the beginning and the end of each segment of the pulse. For example, for the precursor, t_1 is the time at which (for the first time) the pulse appears at the output and t_2 is a time between the precursor and the main signal for which the pulse envelope is minimum (it is not necessarily zero). On the other hand, the main signal starts at the end of the precursor and ends as the signal disappears in the output sampling point. It can be seen from Fig. 9 that the value of U for the main signal is almost 50 times of the one for precursors for the 1DPC with five slabs. As the number of slabs increases, we can say that the energy of the main signal decreases drastically but the rate of attenuation (which is proportional to the energy attenuation rate) for the precursors is lower. For example, in the case of 1DPC with nine slabs, the value of U for the main signal and precursors are relatively comparable (the value of the U for the main signal is three times the value of the U for the precursors). Based on the difference between the attenuation rate of the main part of the signal and the precursors, the following observation can be made. By continuously increasing the number of slabs, the energy of the precursors can theoretically be made higher than the energy of the main part of the signal. It has to be noted though that as the number of slabs becomes greater than 12, both the main part of the signal and the precursors die out, eliminating any clear distinction between themselves. However, the possibility of optimizing the form of the excitation in order to maximize the precursors has been demonstrated for temporally dispersive media, in [32]. The present paper paves the way for a future investigation of similar possibilities for spatially dispersive media.

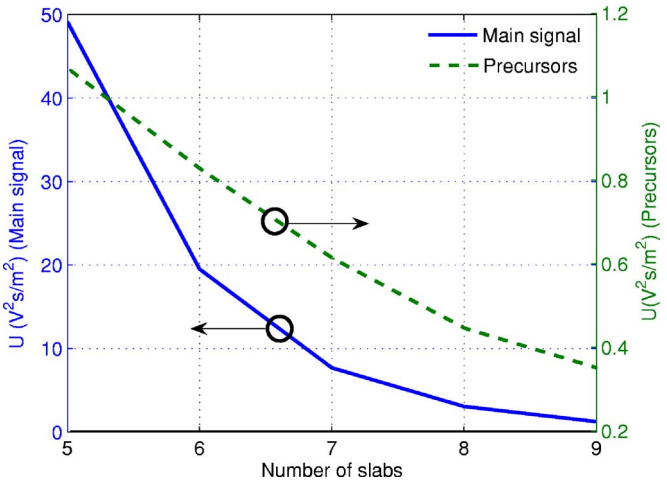

FIG. 9. (Color online) The values of U for the precursor and the main part of the pulse for different number of slabs.

V. SUMMARY AND CONCLUDING REMARKS

This paper describes the time and frequency evolution of a modulated Gaussian pulse in a passive Lorentzian media and a one-dimensional photonic crystal (1DPC) using the finite-difference time-domain (FDTD) and joint time-frequency analysis (JTFA). Time and frequency evolution of the precursors and the fact that their propagation velocity is subluminal has been verified. Despite the claim by the au-

thors in reference [8], asserting that they have demonstrated superluminal information velocity using (smooth) signals by means of under cut-off frequencies and without generating further precursors, this does not seem to be true in practice. In order to send a signal, some discontinuities have to be created that in turn generate new precursors and if the signal cannot overtake its precursors, then information cannot be transmitted faster than light, in spite of the fact that group velocity can be superluminal. An interesting point in these simulations is that the front of the pulse is subluminally delayed as it travels through the structure. Therefore, although the group velocity is superluminal, precursors which are the genuine carriers of information, are not. This work also presents the combination of FDTD and JTFA as a tool that can be used to study both the transient and steady state of the time and frequency evolution of a pulse propagating inside a complex dispersive medium.

ACKNOWLEDGMENTS

This work was supported by the Natural Sciences and Engineering Research Council of Canada under Grant Nos. 249531-02 and 261775-03, and in part by Photonic Research Ontario, Funded Research No. 72022792.

[1] L. Brillouin, *Wave Propagation and Group Velocity* (Academic, New York, 1960).
[2] R. Y. Chiao and A. M. Steinberg, *Progress in Optics*, edited by E. Wolf (Elsevier, Amsterdam, 1997), Vol. 37, pp. 347–406.
[3] M. Mojahedi, E. Schamiloglu, F. Hegeler, and K. J. Malloy, Phys. Rev. E **62**, 5758 (2000).
[4] M. Mojahedi, E. Schamiloglu, K. Agi, and K. J. Malloy, IEEE J. Quantum Electron. **36**, 418 (2000).
[5] A. Ranfagni and D. Mugnai, Phys. Rev. E **54**, 5692 (1996).
[6] A. Ranfagni, D. Mugnai, P. Fabeni, and G. P. Pazzi, Appl. Phys. Lett. **58**, 774 (1991).
[7] D. Mugnai, A. Ranfagni, and L. Ronchi, Phys. Lett. A **247**, 281 (1998).
[8] A. Enders and G. Nimtz, Phys. Rev. B **47**, 9605 (1993).
[9] C. Spielmann, R. Szipocs, A. Stingl, and F. Krausz, Phys. Rev. Lett. **73**, 2308 (1994).
[10] L. J. Wang A. Dogariu, and A. Kuzmich, Nature (London) **406**, 277 (2001).
[11] A. M. Steinberg and R. Y. Chiao, Phys. Rev. A **51**, 3525 (1995).
[12] A. M. Steinberg, P. G. Kwiat, and R. Y. Chiao, Phys. Rev. Lett. **71**, 708 (1993).
[13] J. F. Woodley and M. Mojahedi, Phys. Rev. E **70**, 046603 (2000).
[14] O. F. Siddiqui, S. J. Erickson, G. V. Eleftheriades, and M. Mojahedi, IEEE Trans. Microwave Theory Tech. **52**, 1449 (2004).
[15] M. Born and E. Wolf, *Principles of Optics: Electromagnetic Theory of Propagation, Interference and Diffraction of Light* (Pergamon, New York, 1970), Vol. 4.
[16] L. Brillouin, *Wave Propagation in Periodic Structures; Electric Filters and Crystal Lattices* (McGraw-Hill, New York, 1946).
[17] E. L. Bolda, R. Y. Chiao, and J. C. Garrison, Phys. Rev. A **48**, 3890 (1993).
[18] R. Y. Chiao, Phys. Rev. A **48**, R34 (1993).
[19] E. L. Bolda, J. C. Garrison, and R. Y. Chiao, Phys. Rev. A **49**, 2938 (1994).
[20] R. Y. Chiao and J. Boyce, Phys. Rev. Lett. **73**, 3383 (1994).
[21] K. E. Oughstun and G. C. Sherman, *Electromagnetic Pulse Propagation in Causal Dielectrics* (Springer-Verlag, Berlin Heidelberg, 1994).
[22] C. M. Balictsis and K. E. Oughstun, Phys. Rev. E **47**, 3645 (1993).
[23] A. Taflove and S. C. Hagness, *Computational Electrodynamics-The Finite-Difference Time-Domain Method* (Artech House, 2000).
[24] P. G. Petropoulos, IEEE Trans. Antennas Propag. **42**, 62 (1994).
[25] L. Cohen, *Time-Frequency Analysis* (Prentice Hall, NJ, 1995).
[26] L. Carin, L. B. Felsen, D. Kralj, S. U. Pillai, and W. C. Lee, IEEE Trans. Antennas Propag. **4**, 23 (1994).
[27] A. Moghaddar and E. K. Walton, IEEE Trans. Antennas Propag. **41**, 677 (1993).
[28] J. A. Stratton, *Electromagnetic Theory* (McGraw-Hill, New York, 1941).
[29] M. J. Ablowitz and A. S. Fokas, *Complex Variables: Introduction and Application*, 2nd ed. (Cambridge University Press, Cambridge, 1997).
[30] M. Mojahedi, K. J. Malloy, G. V. Eleftheriades, J. Woodley, and R. Y. Chiao, IEEE J. Sel. Top. Quantum Electron. **9**, 30 (2003).
[31] R. Safian, C. D. Sarris, and M. Mojahedi, Antennas, Radar, and Wave Propagation Conference (IASTED and IEEE AP-S), Banff, Canada (2005).
[32] K. E. Oughstun, IEEE Trans. Antennas Propag. **53**, 1582 (2005).